A Physical Model of FeLoBALs:

Implications for Quasar Feedback

Claude-André Faucher-Giguère

UC Berkeley

Miller Institute for Basic Research in Science

Eliot Quataert & Norm Murray

arXiv:1108:0413

Outline

- What are FeLoBALs?

- A physical model of FeLoBALs:
  - ➡ formation *in situ* at *R*~kpc
    (physically distinct from most, high-ionization BALs)
  - ➡ radiative shocks in cloud crushing

- Implications for QSO feedback

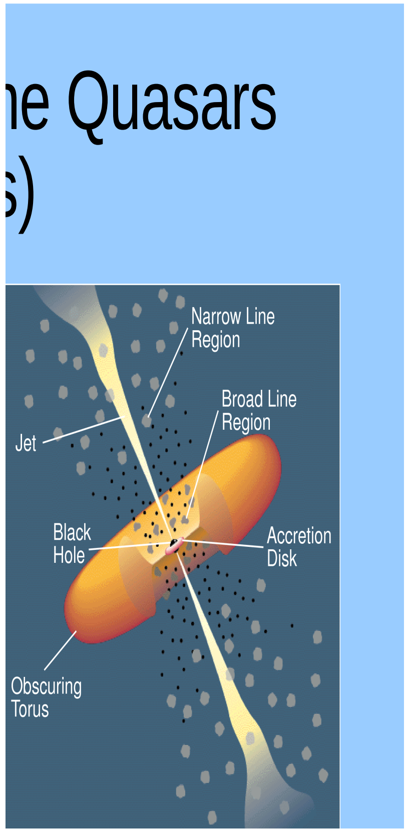

Urry & Padovani 95

What are BALs?

- Broad absorption lines in QSOs:
    - ➡ usually high-ionization SiIV, CIV
    - ➡ blue shifted $v\sim10{,}000$ km/s, $\Delta v\sim1{,}000$s km/s $\Rightarrow$ AGN outflows
    - ➡ $R\lesssim1$ pc (variability) $\Rightarrow$ accretion disk winds (Murray+95)
- Seen in ~20% of QSOs (up to 40% in IR-selected samples)

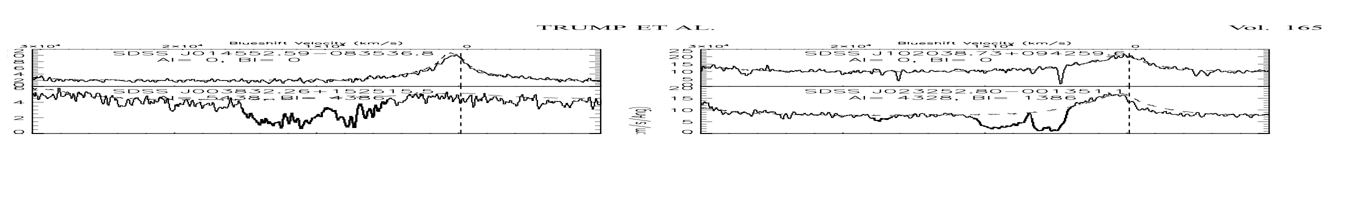

Trump+06

What are FeLoBALs?

- Subset of QSO BALs
  - ➡ absorption by low-ionization species, including FeII
  - ➡ lower *v*~1,000-10,000 km/s, *Δv*~100s km/s
- Rare:
  - ➡ only ~1/500 of optical QSOs have FeLoBALs (~1% in IR)
- No real theory

SDSS J0318-0600

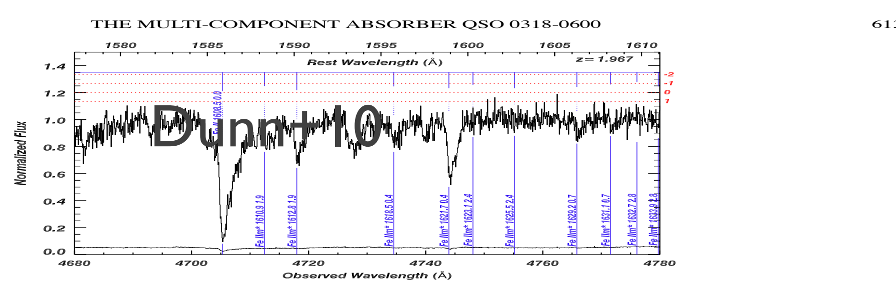

FeLoBALs are particularly well-suited for photoionization modeling

- Fine structure lines of FeII and HeI have orthogonal dependences on n_e and T

- Observations ($L_{bol}=10^{46.7-47.7}$ erg s^{-1}) + photoionization modeling (Cloudy) have revealed (Moe+09, Dunn+10, Bautista+10):

  ➡ $n_e \sim 10^4$ cm^{-3}

  ➡ $T \sim 10^4$ K

  ➡ $N_H \sim 10^{20-21}$ (

  ➡ $R \sim 1$-3 kpc (distance from SMBH)

  ➡ $\Delta R \sim 0.01$ pc (absorber thickness)

⇒ $\Delta R/R \sim 10^{-5}$!!!

n_e diagnostic for QSO 2359-1241

1, 2010 DISTANCE TO MULTIPLE FeLoBAL COMPONENTS 27

Table 2
Measured Column Densities in SDSS J0318–0600

Species	E_{low} (cm^{-1})	Column Density ($\times 10^{12}$ cm^{-2})			
		Comp. **a**	Comp. **i**	Comp. **k**	Comp. **b–h**
Al II	0	116.1 ± 0.1	400 ± 40	35.0 ± 0.3	>390
Al III	0	46.0 ± 0.4	1560 ± 220	73.0 ± 0.8	>810
C II	0	333 ± 11		1100 ± 200	>14000
C II	63	577 ± 21	>19000	1800 ± 300	
C IV	0	734 ± 10	29000 ± 3000	1297 ± 13	>10000
Fe II	0	<40	1275 ± 35	154 ± 6	>490
Fe II	385		294 ± 77		
Fe II	668			9.0 ± 0.3	
Fe II	863		147 ± 36		
Fe II	977				
Fe II	1873		163 ± 49		
Fe II	2430		25.0 ± 5.4		
Fe II	7955		8.1 ± 0.2		
Mg II	0	28.7 ± 0.1	3200 ± 400	192 ± 1	>880
Mn II	0		17.5 ± 0.1		
Ni II	0		180 ± 4	<120	
Ni II	8394		64.0 ± 0.4	10.0 ± 0.3	
Si II	0	101 ± 3	7220 ± 100	640 ± 150	>3500
Si II	287	<50	7380 ± 130	352 ± 12	
Si IV	0	145 ± 6	5600 ± 1300	140 ± 4	>1800

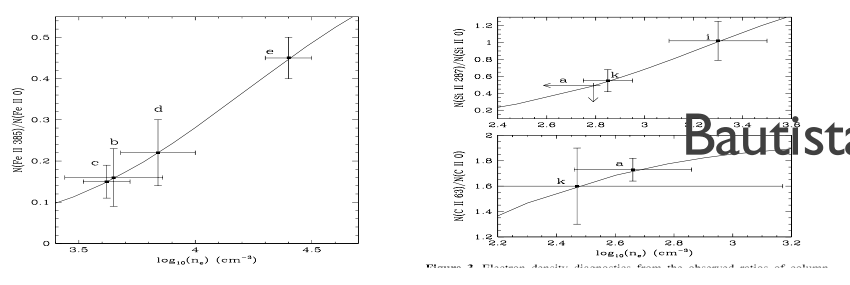

Bautista+10

FeLoBAL must form *in situ*, at *R*~kpc from SMBHs

- If FeLoBALs traveled from the SMBH to their implied location...

$$t_{\rm flow} \approx \frac{R}{v} \approx 3 \times 10^5 \ {\rm yr} \left(\frac{R}{3 \ {\rm kpc}} \right) \left(\frac{v}{10,000 \ {\rm km \ s^{-1}}} \right)^{-1}$$

- But destroyed by hydro instabilities and thermal evaporation in

$$t_{\rm KH} \approx 630 \kappa \ {\rm yr}$$

$$t_{\rm evap} \approx 6 \times 10^3 \ {\rm yr}$$

CAFG, Quataert, & Murray,

Radiative shock model outline

- FeLoBALs can form *in situ* via interaction of a quasar blast wave with an interstellar gas clump

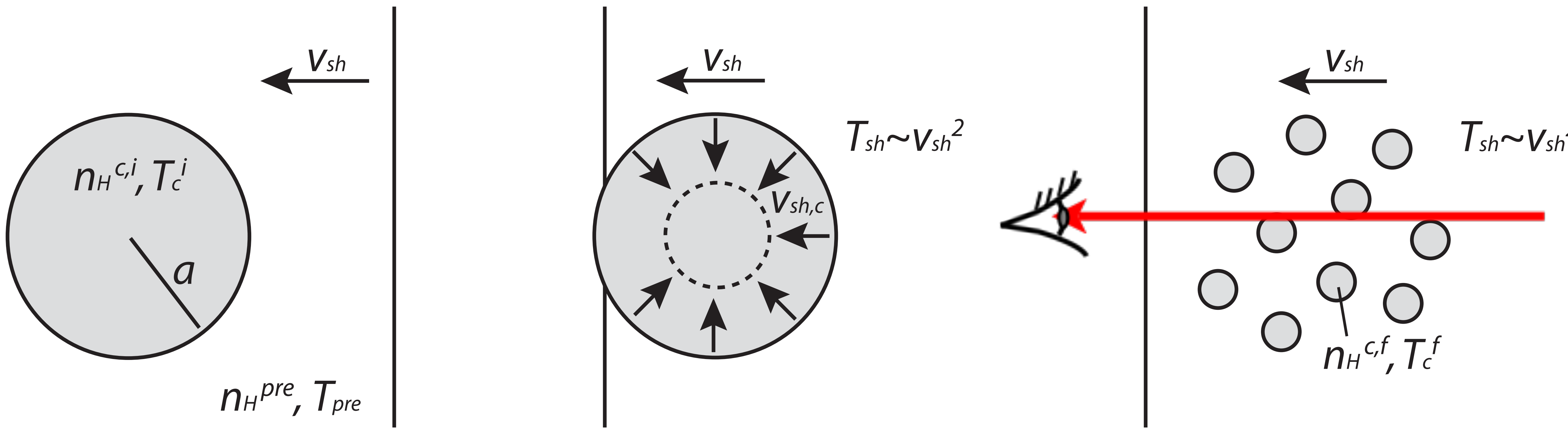

QSO blast wave encounters moderately dense ISM cloud.

Shock wave propagates in cloud on crushing time t_{cc}, cloud is destroyed by K-H in $t_{KH} \sim 20 t_{cc}$, and is accelerated to $\sim v_{sh}$ in t_{drag}.

At $t > t_{KH}$, t_{drag}, original cloud is shredded into cloudlets traveling at $\sim v_{sh}$ and compressed by hot post-shock gas.

CAFG, Quataert, & Murray, submitted

Cloud crushing by shocks, Kelvin-Helmholtz instability

- Well-studied problem for SNRs (e.g., Klein+94, Mellema+02, Cooper+09)

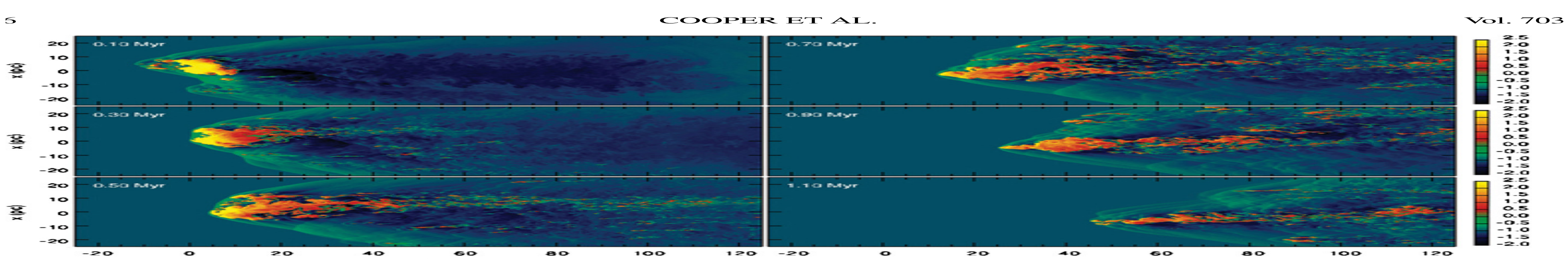

$$v_{\rm sh,c} \approx v_{\rm sh}\sqrt{\frac{n_{\rm H}^{\rm ext}}{n_{\rm H}^{\rm c}}} \qquad t_{\rm cc} \approx \frac{\Delta R}{2 v_{\rm sh,c}} \qquad t_{\rm KH} \sim \kappa t_{\rm cc}$$

CAFG, Quataert, & Murray, submitted

Requirements for producing FeLoBALs in radiative shocks explain observed properties

- Acceleration, cold gas:

$$t_{\rm drag} < t_{\rm KH} \quad t_{\rm cool} < t_{\rm cc} \quad \Rightarrow N_{\rm H} \gtrsim 10^{20}\ {\rm cm}^{-2} \left(\frac{v_{\rm sh}}{5,000\ {\rm km\ s}^{-1}} \right)^{4.2}$$

- Post-shock compression:

$$n_{\rm H}^{\rm BAL} \approx 4 n_{\rm H}^{\rm pre} \left(\frac{T_{\rm sh}}{10^4\ {\rm K}} \right) \sim 10^4\ {\rm cm}^{-3}$$

$$\Rightarrow \Delta R \sim 0.01\ {\rm pc}$$

CAFG, Quataert, & Murray,

Other FeLoBAL model successes

- FeII selects $U_{\rm H} \propto L_{\rm bol}/R^2 n_{\rm H}^{\rm BAL} \sim 10^{-3} - 10^{-2}$

⇒ R~kpc in bright L_{bol}=$10^{46.7\text{-}47.7}$ erg s^{-1} QSOs analyzed

- Shredding of ISM clump

⇒ multiple components at same *R*, but different *v*

⇒ supra-thermal line widths

BAUTISTA ET AL. Vol. 713

Table 1
Measured Column Densities in QSO 2359–1241

Species	$E_{\rm low}$ (cm^{-1})	Column Density ($\times 10^{12}$ cm^{-2})				
		Comp. **a**	Comp. **b**	Comp. **c**	Comp. **d**	Comp. **e**
He I	159 856	14.3 ± 0.7	22.9 ± 3.4	6.1 ± 0.3	4.5 ± 2.2	138.0 ± 9.9
Fe II	0	0.49 ± 0.08	5.7 ± 1.5	2.7 ± 0.3	2.7 ± 0.1	72.4 ± 3.5
Fe II	385		0.93 ± 0.28	0.40 ± 0.09	0.60 ± 0.22	32.4 ± 1.2
Fe II	668		1.1 ± 0.5			18.2 ± 1.3
Fe II	863		0.45 ± 0.20			11.5 ± 0.9
Fe II	977					7.1 ± 0.6
Fe II	1873					77.6 ± 9.5
Fe II	7955					5.0 ± 0.5
Mg I	0	0.04 ± 0.02	2.1 ± 1.0	0.28 ± 0.02	0.04 ± 0.03	0.83 ± 0.06
Mg II	0					>65
Si II	0		198 ± 48			
Si II	287					794 ± 206
Al III	0			12.7 ± 0.4		>79
Ca II	0	0.07 ± 0.03	0.83 ± 0.04	0.47 ± 0.02		3.3 ± 0.3
Ni II	8394					6.2 ± 0.6

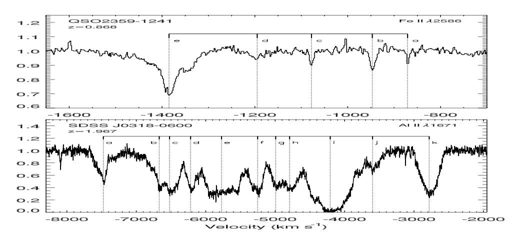

to-noise data allowed us to measure the column densities from 5 unblended absorbers in QSO 2359–1241 and 11 components in SDSS J0318–0600. For the latter, though, only the strongest components, **a**, **i**, and **k**, could be independently measured, while all other components had to be measured as a single blended structure. Whenever possible, the column de[illegible]ities were de-termined through three different assumptions [illegible] ing or apparent optical depth, partial line-of-si[illegible] velocity-dependent covering according to the p[illegible] of de Kool et al. (2001) and Arav et al. (2005). For each component in QSO 2359–1241, we find that the troughs require the power-law method to determine the full column density. We quote the column density determined by the power-law method in Table 1. For the three components in SDSS J0318–0600, we find that the results of these three methods are generally in good agreement, indicating that there is full covering of each source and the column densities could be reliably measured (see Dunn et al. 2010). The measured column densities for the observed components in QSO 2359–1241 and SDSS J0318–0600 are given in Tables 1 and 2, respectively.

Bautista+10

- Dust in clump ⇒ FeLoBAL QSOs are redder than average

CAFG, Quataert, & Murray,

Implications for QSO feedback

- Not a cold, thin shell outflow!

- Most of kinetic power in hot flow:

$$\dot{M}_{\rm hot} = 8\pi\Omega_{\rm hot} R N_{\rm H}^{\rm hot} \mu m_{\rm p} v_{\rm hot}$$

- Can be estimated from FeLoBALs assuming v_{hot}~v and pressure eq.

$$\Rightarrow \dot{E}_{\rm k} \approx 2-5\%\ L_{\rm bol}$$

$$\dot{P} \approx 2-10\ L_{\rm bol}/c$$

$$\dot{M} \approx 1,000-2,000\ {\rm M}_\odot\ {\rm yr}^{-1}$$

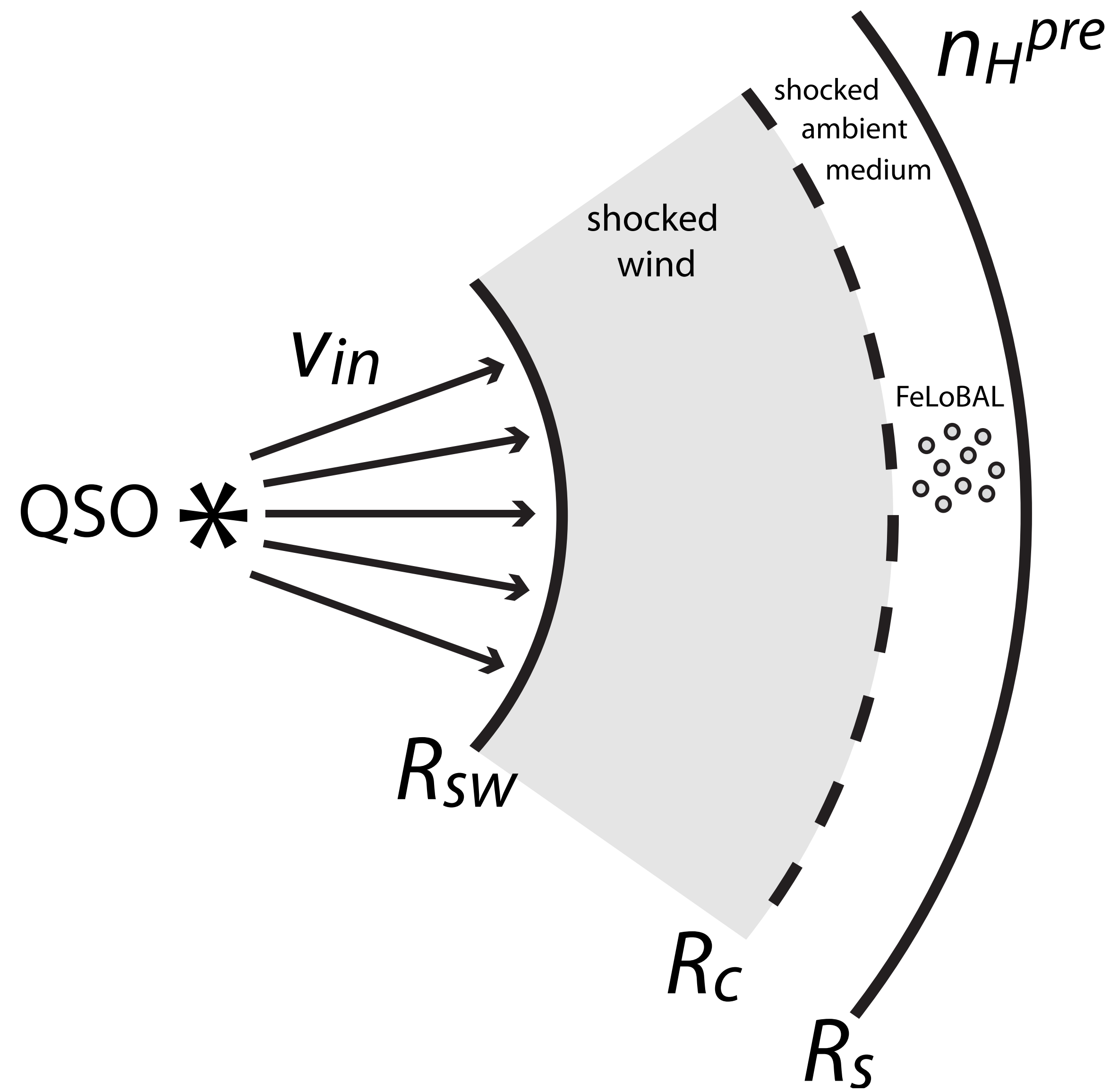

CAFG, Quataert, & Murray,

FeLoBAL energetics agree well with molecular outflows in ULIRGs

- Recent observations of outflows in local ULIRGs also indicate $\dot{E}_{\mathrm{K}} \sim \text{few } \% \; L_{\mathrm{bol}}(\mathrm{AGN})$

  (Feruglio+10, Fischer+10, Sturm+11, Rupke & Veilleux 11)

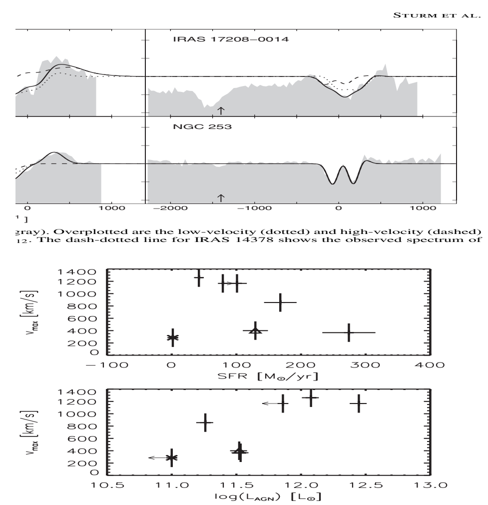

- FeLoBALs may be analogous galaxy-scale AGN outflows in later ('blow out') evolutionary stage

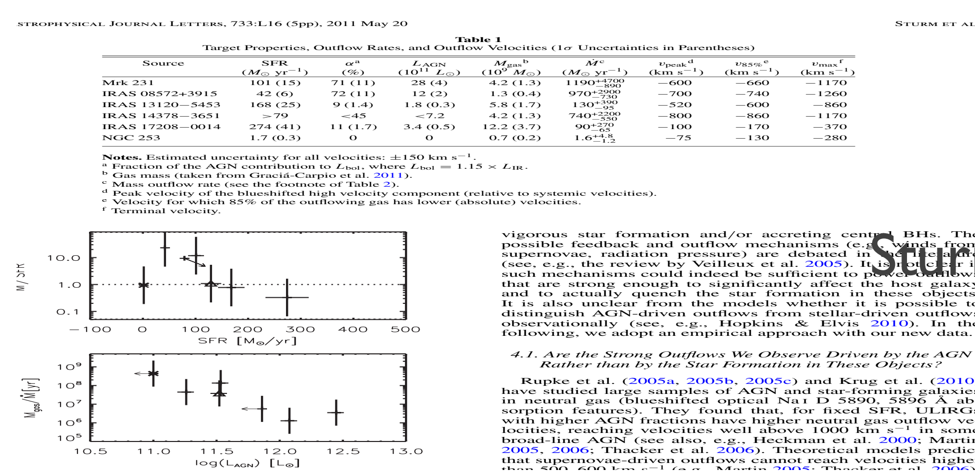
strophysical Journal Letters, 733:L16 (5pp), 2011 May 20 — Sturm et al.

Table 1
Target Properties, Outflow Rates, and Outflow Velocities (1σ Uncertainties in Parentheses)

Source	SFR ($M_\odot$ yr^{-1})	α[a] (%)	L_{AGN} (10^{11} $L_\odot$)	M_{gas}[b] (10^9 $M_\odot$)	$\dot{M}$[c] ($M_\odot$ yr^{-1})	v_{peak}[d] (km s^{-1})	$v_{85\%}$[e] (km s^{-1})	v_{max}[f] (km s^{-1})
Mrk 231	101 (15)	71 (11)	28 (4)	4.2 (1.3)	1190^{+4700}_{-890}	−600	−660	−1170
IRAS 08572+3915	42 (6)	72 (11)	12 (2)	1.3 (0.4)	970^{+2900}_{-730}	−700	−740	−1260
IRAS 13120−5453	168 (25)	9 (1.4)	1.8 (0.3)	5.8 (1.7)	130^{+390}_{-95}	−520	−600	−860
IRAS 14378−3651	>79	<45	<7.2	4.2 (1.3)	740^{+2200}_{-550}	−800	−860	−1170
IRAS 17208−0014	274 (41)	11 (1.7)	3.4 (0.5)	12.2 (3.7)	90^{+270}_{-65}	−100	−170	−370
NGC 253	1.7 (0.3)	0	0	0.7 (0.2)	$1.6^{+4.8}_{-1.2}$	−75	−130	−280

Notes. Estimated uncertainty for all velocities: ±150 km s^{-1}.
[a] Fraction of the AGN contribution to L_{bol}, where $L_{bol} = 1.15 \times L_{IR}$.
[b] Gas mass (taken from Graciá-Carpio et al. 2011).
[c] Mass outflow rate (see the footnote of Table 2).
[d] Peak velocity of the blueshifted high velocity component (relative to systemic velocities).
[e] Velocity for which 85% of the outflowing gas has lower (absolute) velocities.
[f] Terminal velocity.

vigorous star formation and/or accreting cent[illegible] BHs. The possible feedback and outflow mechanisms (e.g[illegible] winds from supernovae, radiation pressure) are debated in [illegible] (see, e.g., the review by Veilleux et al. 2005). It is [illegible] such mechanisms could indeed be sufficient to po[illegible] that are strong enough to significantly affect the host galaxy and to actually quench the star formation in these objects. It is also unclear from the models whether it is possible to distinguish AGN-driven outflows from stellar-driven outflows observationally (see, e.g., Hopkins & Elvis 2010). In the following, we adopt an empirical approach with our new data.

4.1. Are the Strong Outflows We Observe Driven by the AGN Rather than by the Star Formation in These Objects?

Rupke et al. (2005a, 2005b, 2005c) and Krug et al. (2010) have studied large samples of AGN and star-forming galaxies in neutral gas (blueshifted optical Na I D 5890, 5896 Å absorption features). They found that, for fixed SFR, ULIRGs with higher AGN fractions have higher neutral gas outflow velocities, reaching velocities well above 1000 km s^{-1} in some broad-line AGN (see also, e.g., Heckman et al. 2000; Martin 2005, 2006; Thacker et al. 2006). Theoretical models predict that supernovae-driven outflows cannot reach velocities higher

Sturm+11

Summary

- FeLoBALs probe QSO outflows
- Radiative shock, cloud crushing model explains all the observed FeLoBAL properties (not regular BALs / disk winds!)
- Model + observations $\Rightarrow \dot{E}_{\rm k} \approx 2 - 5\% \; L_{\rm bol}$
- Provides support for (sub-resolution) M-σ models
- Energetics consistent with ULIRG molecular outflows

Extra Slides

In principle, can derive mechanical properties of the QSO wind

- Common assumption of partial, cold thin shell (e.g., Arav 10)

$$\dot{M}_{\rm shell} = 8\pi\Omega R N_{\rm H}^{\rm BAL}\mu m_{\rm p} v \qquad \dot{E}_{\rm k} = \frac{1}{2}\dot{M}_{\rm shell} v^2$$

$\Rightarrow \dot{E}_{\rm K} \sim 0.05 - 1\%\ L_{\rm bol}$ for Ω=0.2 (Moe+09, Dunn+10, Bautista+10)

- But:

➡ can we understand the implied FeLoBAL properties (esp., $\Delta R/R \sim 10^{-5}$)?

➡ what is the proper way of relating the observations to

The possible roles of AGN feedback

Establish correlations between SMBH and galaxy properties

Truncate star formation

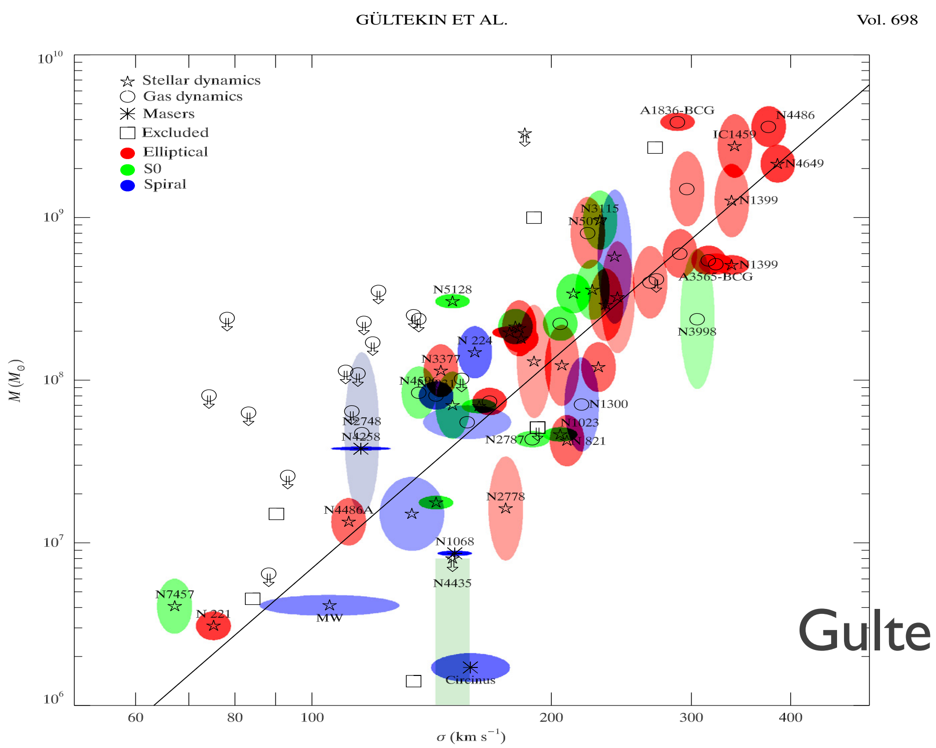

Gultekin+09

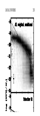

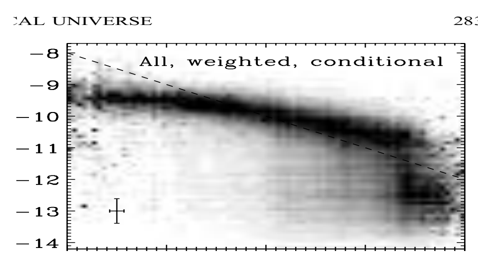

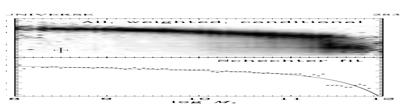

Salim+07

Also, prevent gas cooling in massive halos (“radio mode”)

Prescription-based model successes

- If f~5% of L_{bol} couples to the ISM, then simulations can reproduce the M-σ relation and truncate star formation

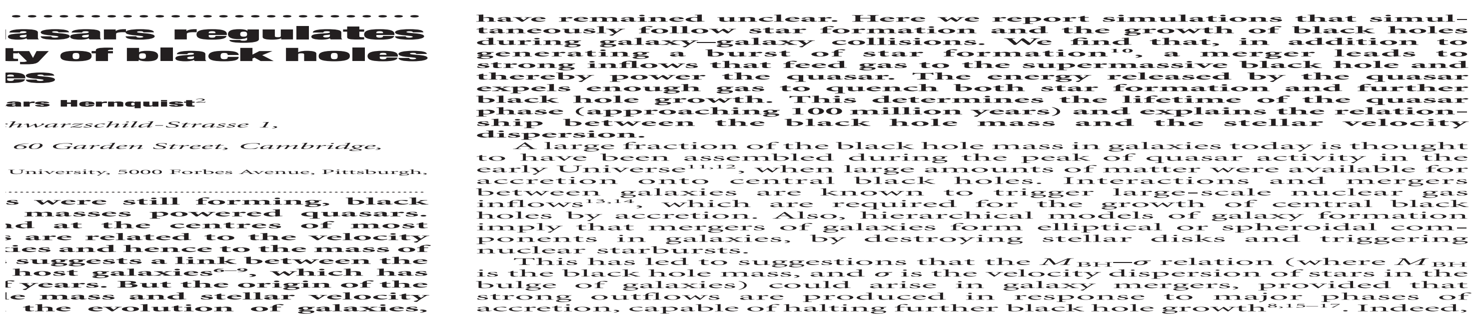

have remained unclear. Here we report simulations that simultaneously follow star formation and the growth of black holes during galaxy–galaxy collisions. We find that, in addition to generating a burst of star formation[10], a merger leads to strong inflows that feed gas to the supermassive black hole and thereby power the quasar. The energy released by the quasar expels enough gas to quench both star formation and further black hole growth. This determines the lifetime of the quasar phase (approaching 100 million years) and explains the relationship between the black hole mass and the stellar velocity dispersion.

A large fraction of the black hole mass in galaxies today is thought to have been assembled during the peak of quasar activity in the early Universe[11,12], when large amounts of matter were available for accretion onto central black holes. Interactions and mergers between galaxies are known to trigger large-scale nuclear gas inflows[13,14], which are required for the growth of central black holes by accretion. Also, hierarchical models of galaxy formation imply that mergers of galaxies form elliptical or spheroidal components in galaxies, by destroying stellar disks and triggering nuclear starbursts.

This has led to suggestions that the M_{BH}–σ relation (where M_{BH} is the black hole mass, and σ is the velocity dispersion of stars in the bulge of galaxies) could arise in galaxy mergers, provided that strong outflows are produced in response to major phases of accretion, capable of halting further black hole growth[8,15–17]. Indeed,

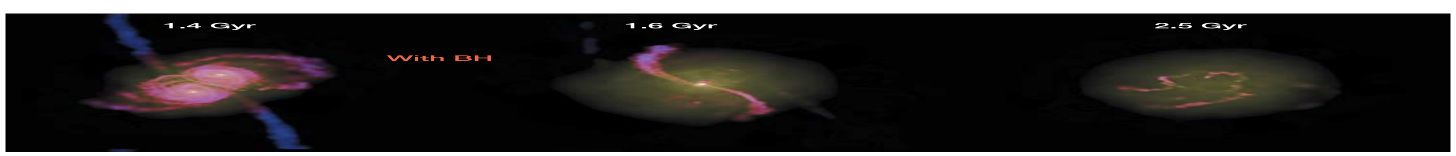

- But, poor understanding of coupling mechanisms & scarce observational constraints

Silk, Rees, Springel, Di Matteo, Hernquist, Hopkins, Wyithe, Loeb, ...